

Article

Magnetically Separable and Recyclable Fe₃O₄-Supported Ag Nanocatalysts for Reduction of Nitro Compounds and Selective Hydration of Nitriles to Amides in Water

Hyunje Woo ¹, Kyoungho Lee ¹, Sungkyun Park ² and Kang Hyun Park ^{1,*}

¹ Department of Chemistry and Chemistry Institute for Functional Materials, Pusan National University, Busan 609-735, Korea; E-Mails: hjwoo@chemistry.or.kr (H.W.); kyoungho@chemistry.or.kr (K.L.)

² Department of Physics, Pusan National University, Busan 609-735, Korea; E-Mail: psk@pusan.ac.kr

* Author to whom correspondence should be addressed; E-Mail: chemistry@pusan.ac.kr; Tel.: +82-51-510-2238; Fax: +82-51-980-5200.

Received: 28 November 2013; in revised form: 27 December 2013 / Accepted: 30 December 2013 / Published: 7 January 2014

Abstract: As hybrid nanostructures have become more important in many fields of chemistry, Ag nanoparticles (NPs) are being increasingly immobilized onto Fe₃O₄ microspheres *in situ*. Structural characterization reveals that the Ag NPs are uniformly immobilized in the Fe₃O₄ microsphere-based supports. Moreover, Ag NPs are more stable in the hybrid structure than in the naked state and show high catalytic activity for the reduction of nitro compounds and hydration of nitriles to amides in water. The Fe₃O₄ microspheres were recycled several times using an external magnet.

Keywords: silver; Fe₃O₄ support; reduction; hydration; magnetic separation

1. Introduction

In recent years, numerous attempts have been made toward designing and synthesizing hybrid nanostructures, which combine or even improve the physical and chemical properties of the constituent parts [1]. Many studies have discussed the syntheses of these multicomponent nanostructures with increased functionality [2,3]. The presence of multicomponent functions combined with the enhanced chemical and physical properties make hybrid nanostructures suitable for research fields pertaining to

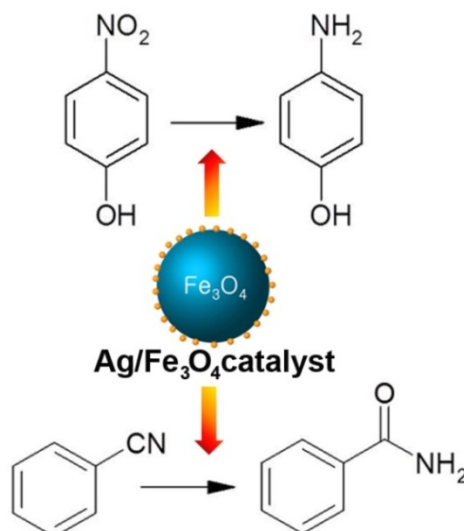
the study of magnetic, plasmonic, and semiconducting properties [4]. Metal NPs immobilized onto metal oxide supports can be used as catalysts in organic reactions, wherein they show higher catalytic activity than the naked metal NPs because of electron transfer across the interface [5–8].

Among the existing metal oxide supports, Fe_3O_4 has gained significance owing to its nanostructure and cutting-edge technological applications, including its usage as a magnetic storage medium [9], in biosensors [10], as well as medical applications such as targeted drug delivery [11,12]. Furthermore, Fe_3O_4 microspheres have been used as supports for the immobilization of metal NPs in nanocatalysis because of the ease of their recyclability using external magnets after the reactions [13].

Recently, many researchers have described the preparation of Ag NPs and studied their various applications in highly active surface-enhanced Raman scattering substrates [14], antibacterial coatings [15], electrochemical and biosensors [16], and as efficient catalysts for organic reactions [17]. A significant number of studies on the catalytic reactions of Ag NPs have been conducted, such as alcohol dehydrogenation, oxidation of phenylsilanes, reduction of aromatic compounds, and Diels-Alder cycloadditions [17–20]. However, during a reaction, the highly active surface atoms destabilize the NPs. To overcome this problem, metal NPs have been immobilized onto supports to increase the stability of the catalysts [21,22].

4-Nitrophenol (Scheme 1) is considered to be one of the most refractory pollutants in wastewaters generated by industrial sources such as companies that manufacture explosives and dyes [23,24]. Due to the importance of 4-aminophenol, there have been many reports about applications of Ag nanoparticles on various supports as catalysts for the reduction of 4-nitrophenol [25–27]. Among them, the use of water as a solvent under mild conditions has attracted much attention in the environmental field. Also, the hydration of nitriles to yield the corresponding amides is of tremendous significance to researchers in academia and industry alike because the resulting amides have numerous applications in synthetic organic and pharmaceutical chemistry. Among various heterogeneous nanocatalysts, supported Ag NPs have been used for this reaction as catalyst [28,29]. In our earlier work, Ag NPs were also used as catalysts for the hydration of nitriles to amides [30].

Scheme 1. Reduction of a nitro compound and hydration of a nitrile to an amide catalyzed by Ag/ Fe_3O_4 catalyst.



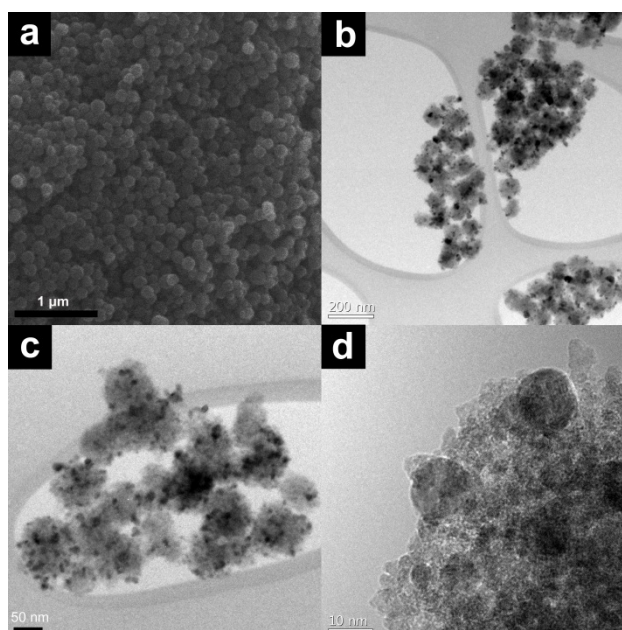
In this paper, Ag NP, immobilized onto Fe₃O₄ microspheres were synthesized and tested as a catalyst in reduction of nitro compounds and nitrile hydration reactions in water (Scheme 1). The monodisperse Ag NPs were easily immobilized without any pretreatment such as attaching functional groups onto the Fe₃O₄ microspheres. This catalyst showed increased Ag NP stability and could be easily recycled using an external magnet after the completion of the reaction.

2. Results and Discussion

2.1. Catalyst Preparation and Characterization

The Fe₃O₄ microspheres were synthesized using the solvothermal method [31]. The partial reduction of FeCl₃ was done at 200 °C using ethylene glycol as a solvent, sodium acetate as a reducing agent, and Na₃Cit as an electrostatic stabilizer. No pretreatment procedures such as attaching functional groups and coating polymers or carbon onto Fe₃O₄, were required prior to the immobilization of Ag NPs onto the Fe₃O₄ microspheres. In fact, Ag NPs were easily immobilized on the surface of Fe₃O₄ *in situ* because of the interaction between the Fe atoms and carboxyl groups of Na₃Cit with Ag. Figure 1 illustrates the morphology of the Ag/Fe₃O₄ catalyst. Figure 1a shows a scanning electron microscopy (SEM) image of spherical Fe₃O₄ microspheres. The immobilized Ag NPs on Fe₃O₄ microspheres were observed in the transmission electron microscopy (TEM) images (Figure 1b–d). The X-ray diffractometer (XRD) pattern of the Ag/Fe₃O₄ and reused Ag/Fe₃O₄ microspheres corresponded to a cubic spinel structure of Fe₃O₄ (JCPDS No. 19-0629) and face-centered cubic of Ag (JCPDS No. 04-07831) (Figure 2a).

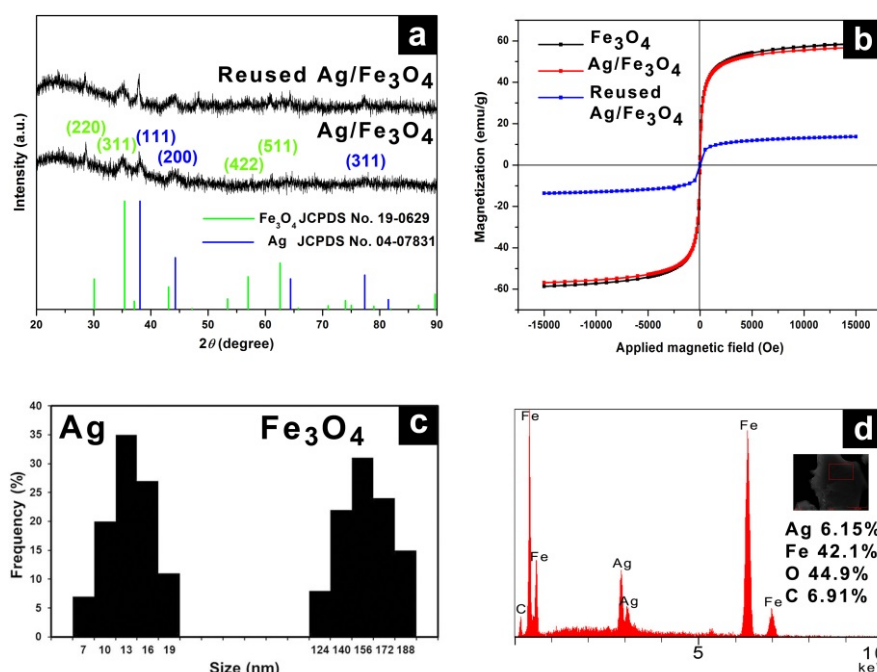
Figure 1. (a) SEM image of Fe₃O₄ microspheres; (b,c) TEM images of Ag/Fe₃O₄; and (d) Immobilized Ag NPs onto Fe₃O₄ microspheres.



In particular, the crystalline pattern was assigned to the (220), (311), (422) and (511) reflections of Fe₃O₄ and (111), (200) and (311) reflections of Ag. The superconducting quantum interference device (SQUID) results in Figure 2b shows the magnetic curves as a function of the applied field at 300 K.

The saturation magnetization value of Ag/Fe₃O₄ was 58.7 emu·g⁻¹, which was similar to that of the Fe₃O₄ microspheres (56.9 emu·g⁻¹). The small decrease of the magnetization value of Ag/Fe₃O₄ microspheres compared to that of Fe₃O₄ microspheres can be attributed to the slight increase of mass due to the immobilized Ag nanoparticles on the surface of Fe₃O₄ microspheres [32]. After hydration, the saturated magnetization value was decreased to 13.7 emu·g⁻¹. Moreover, both the remanence (Mr) and coercivity (Hc) of Fe₃O₄ microspheres were close to zero, indicating superparamagnetism. The average diameters of Fe₃O₄ microspheres and Ag NPs were 150 nm and 12 nm, respectively, as determined from the TEM images (Figure 2c). The elemental compositions of Ag/Fe₃O₄ catalysts were obtained using energy-dispersive X-ray spectroscopy (EDS), showing Ag content (atomic: 6.15% and weight: 17 wt%) (Figure 2d).

Figure 2. (a) XRD pattern of Ag/Fe₃O₄ and reused Ag/Fe₃O₄; (b) SQUID data; (c) Size distributions of Ag NPs and Fe₃O₄ microspheres; and (d) EDS spectrum of Ag/Fe₃O₄.



2.2. Reaction Tests

2.2.1. Reduction of Nitro Compounds

As shown in Figure 3a, the UV/Vis spectrum of the reaction mixture was monitored with time during the catalytic reduction of 4-nitrophenol. Specifically, the absorption of 4-nitrophenol at 400 nm decreases rapidly with a concomitant increase in the peak at 300 nm, which is attributed to the reduction product, 4-aminophenol. The control experiments, where only Fe₃O₄ microspheres were used as the catalyst, showed no reaction (entry 1, Table 1). In the absence of NaBH₄, Ag/Fe₃O₄ catalyst showed no catalytic activity (entry 2, Table 1). As expected, increasing the number of equivalents of NaBH₄ increased the catalytic activity (entries 3–5, Table 1). As shown in Figure 3b, the reaction rate constant *k* is compared under different temperatures at 2.0 mol% of Ag/Fe₃O₄ and 50 equiv. of NaBH₄. The highest catalytic efficiency (0.924 min⁻¹) was obtained at 35 °C.

Figure 3. (a) Time-dependent UV/vis absorption spectra for the reduction of 4-nitrophenol over hybrid Ag/Fe₃O₄ catalyst in aqueous media at 303 K (NaBH₄: 50 equiv.); and (b) Plot of ln(C_t/C₀) versus time for the reduction of 4-nitrophenol over hybrid Ag/Fe₃O₄ catalysts under different temperatures at 2.0 mol% of catalyst and 50 equiv. of NaBH₄.

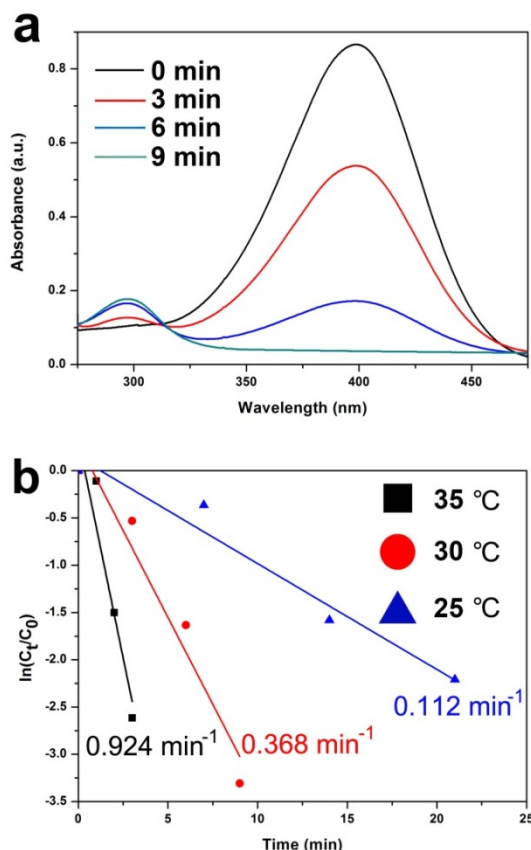
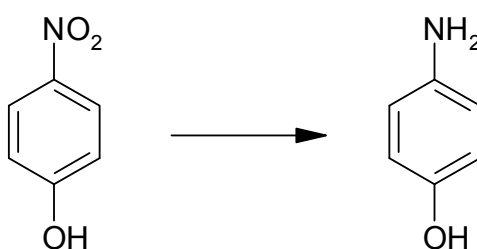


Table 1. Optimization of reaction conditions.



Entry	Catalyst (mol%)	Temp. (°C)	NaBH ₄ (equiv.)	Time	TOF (h ⁻¹)
1	Fe ₃ O ₄ (2.0)	25	300	4 h	No reaction
2	Ag/Fe ₃ O ₄ (2.0)	25	0	4 h	No reaction
3	Ag/Fe ₃ O ₄ (2.0)	25	50	20 min	150
4	Ag/Fe ₃ O ₄ (2.0)	25	200	3 min	1000
5	Ag/Fe ₃ O ₄ (2.0)	25	300	4 min 10 s	1059
6	Ag/Fe ₃ O ₄ (2.0)	25	300	2 min 5 s	1440

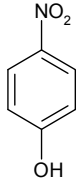
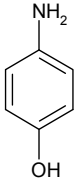
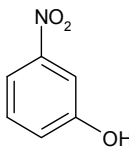
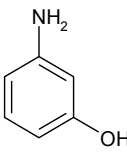
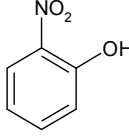
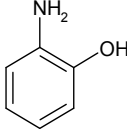
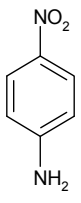
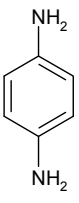
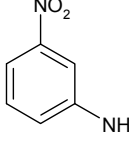
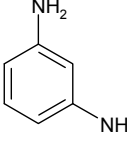
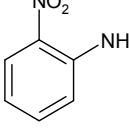
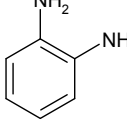
Reaction conditions: 10 mL of 7.50×10^{-4} M 4-nitrophenol, 0.026 mg of Ag/Fe₃O₄ [Ag base (17 wt%): 2.0 mol%], 1.0 mL of 2.22 M NaBH₄ (300 equiv. to the substrate).

We then sought to optimize reaction temperature during the reduction (entries 5 and 6, Table 1). The reduction was finished in 2 min 5 s where Ag/Fe₃O₄ was used as the catalyst (2.0 mol% of

catalyst, 300 equiv. of NaBH₄ per equiv. substrate). Ag/Fe₃O₄ catalyst exhibited superior catalytic activity to previous reported Ag/halloysite nanocomposites and Ag nanoshell-coated cationic polystyrene beads in the comparison with turnover frequency (TOF) value [33,34].

We also confirmed the catalytic activity of hybrid Ag/Fe₃O₄ for the reduction of other nitroarene analogues (Table 2). As shown in Table 2, we found that our Ag/Fe₃O₄ catalyst promoted high reactivities and excellent yields for a series of model nitrophenols and aniline compounds, regardless of the types and positions of the substituents.

Table 2. Reduction of various nitroarenes using hybrid Ag/Fe₃O₄ catalyst.

Entry	Substrate	Product	Time	TOF (h ⁻¹)
1			2 min 5 s	1440
2			1 min 40 s	1800
3			6 min 50 s	439
4			6 min	500
5			5 min 40 s	529
6			18 min 20 s	164

Reaction conditions: 10 mL of 7.50×10^{-4} M 4-nitrophenol, 0.026 mg of Ag/Fe₃O₄ [Ag base (17 wt%): 2.0 mol%], 1.0 mL of 2.22 M NaBH₄ (300 equiv. to the substrate) at 308 K.

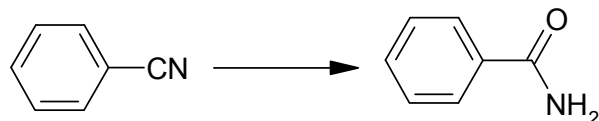
Interestingly, when the reductions of 4-, 3-, and 2-nitrophenols were catalyzed by Ag/Fe₃O₄, the 4- and 3-nitrophenol reductions showed better activities than that of 2-nitrophenol because of a steric

effect (entries 1–3, Table 2). Remarkably, the TOF in Entry 2 is $1,800 \text{ h}^{-1}$, which is calculated using the moles of nitroarene consumed per mole of the hybrid $\text{Ag}/\text{Fe}_3\text{O}_4$ catalyst for a reaction time of 1 h under the present reaction condition. Interestingly, *m*-nitro compounds exhibited better conversion efficiencies than other nitro compounds because of a resonance effect (entries 4–6, Table 2).

2.2.2. Hydration of Nitriles to Amides

The reaction of benzonitrile in water was chosen as the test model. A possible mechanism of nitrile hydration by Ag catalyst is shown by Satsuma's group [28]. Almost no reaction occurred in the absence of a catalyst (entry 1, Table 3). Generally, time, temperature, and quantity of catalyst are important considerations for increasing rate of the conversion. A 2% conversion was obtained at $100 \text{ }^\circ\text{C}$ within 2 h of the reaction in the presence of 1.0 mol% catalyst (entry 2, Table 3). When the temperature was increased to $150 \text{ }^\circ\text{C}$, 25% conversion was achieved within the same reaction time, *i.e.*, 2 h (entry 3, Table 3). As mentioned in entry 4, the conversion increased slightly within 6 h of the reaction. Finally, the optimum reaction conditions were found to be as follows: nitrile (0.1 mL, 1.0 mmol) with $\text{Ag}/\text{Fe}_3\text{O}_4$ (19.0 mg, 3.0 mol%) in H_2O (3.0 mL) in a stainless steel reactor (entry 5, Table 3). Under these conditions, $\text{Ag}/\text{Fe}_3\text{O}_4$ catalyst showed better catalytic activity than a previously reported SiO_2 -supported Ag nanocatalyst [28]. 27% conversion was obtained with a reaction time of 6 h at $120 \text{ }^\circ\text{C}$ (entry 6, Table 3).

Table 3. Optimization of reaction conditions.



Entry	Catalyst (mol%)	Temp. ($^\circ\text{C}$)	Time (h)	Conversion ^a (%)
1	Blank	150	6	8
2	1	100	2	2
3	1	150	2	25
4	1	150	6	36
5	3	150	6	>99
6	3	120	6	27
7	2	150	6	85
8	3	150	1	31
9	Recovered from #5	150	6	>99
10	Recovered from #9	150	6	>99
11	Recovered from #10	150	6	>99

^a Determined by using gas chromatography-mass spectrometry (GC-MS) spectroscopy. *Reaction conditions:* nitriles (1.0 mmol), $\text{Ag}/\text{Fe}_3\text{O}_4$ catalyst (3.0 mol%), H_2O (3.0 mL).

Interestingly, the conversion decreased only slightly when 2.0 mol% $\text{Ag}/\text{Fe}_3\text{O}_4$ was used (entry 7, Table 3). As expected, lowering the reaction time effectively decreased the conversion (entry 8, Table 3). Among the three factors of reaction time, temperature, and quantity of catalyst, we found that the reaction temperature was the most important because the conversion decreased drastically at $120 \text{ }^\circ\text{C}$ (entries 5 and 6, Table 3). Remarkably, the $\text{Ag}/\text{Fe}_3\text{O}_4$ catalysts were easily separated using an external

magnet (Scheme 2) after the completion of the reaction, and reused three times under the same reaction conditions without any loss of catalytic activity (entries 9–11, Table 3). As shown in Figure 4, the structure of the Ag/Fe₃O₄ microspheres remained unchanged after the reaction ended, thereby demonstrating catalyst recyclability.

Scheme 2. Magnetic separation and recycling of the Ag/Fe₃O₄ catalyst.

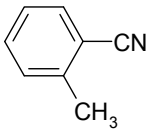
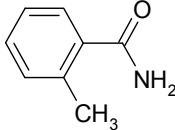
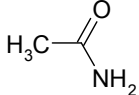
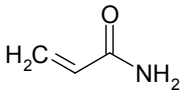


The optimized reaction conditions determined for the Ag/Fe₃O₄ catalyst system were applied to various other substituents (Table 4).

Table 4. Hydration of various nitriles catalyzed by Ag/Fe₃O₄ catalyst.

Entry	Substrate	Product	Yield ^a (%)
1			>99
2			96
3			60
4			40
5			98
6			86

Table 4. Cont.

Entry	Substrate	Product	Yield ^a (%)
7			13
8	H ₃ C—CN		>99
9	H ₂ C=CH—CN		87

^a Determined by using GC-MS Spectroscopy. Reaction conditions: nitriles (1.0 mmol), Ag/Fe₃O₄ catalyst (3.0 mol%), H₂O (3.0 mL), 150 °C, 6 h.

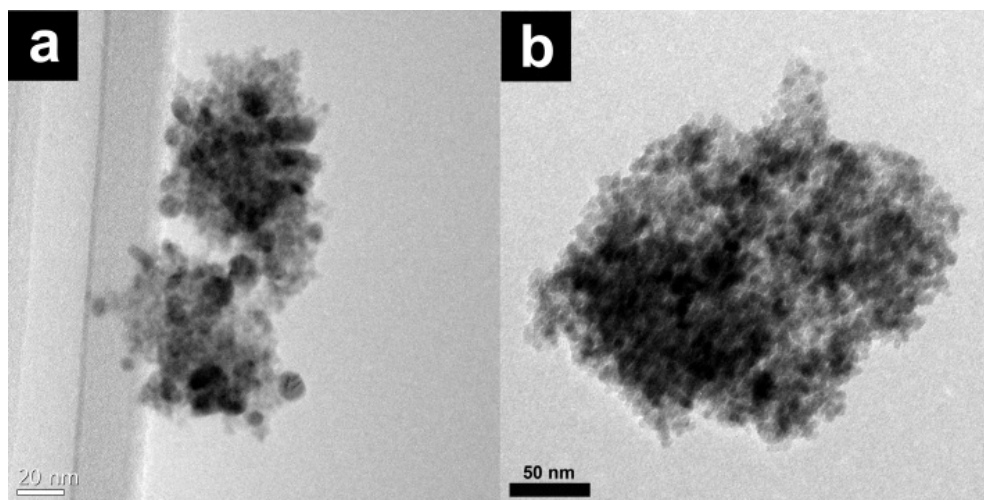
We confirmed that this reaction could be extended to a wide variety of nitriles. The reaction rates were not influenced substantially by the electronic effects of the substituents on the aromatic rings of nitriles. Both, 4-chlorobenzonitrile and 4-bromobenzonitrile showed high conversions of more than 95% (entries 1 and 2, Table 4). The nitro and amino groups on the nitrile were less active than the halide substituents (entries 3 and 4, Table 4). When the hydration of *o*-, *m*-, and *p*-tolunitriles was catalyzed by Ag/Fe₃O₄, steric effects of *ortho*-substituted nitriles on the reaction rates were observed (entries 5–7, Table 4). The hydration of aliphatic nitriles such as acetonitrile and acrylonitrile was also accomplished with high conversions (entries 8 and 9, Table 4)

3. Experimental

3.1. General Remarks

The morphology of each sample was characterized by TEM (FEI, Tecnai F30 Super-Twin) located at the National Nanofab Center (Daejeon, South Korea) by placing a few drops of the corresponding colloidal solution on carbon-coated copper grids (200 mesh, F/C coated, Ted Pella Inc., Redding, CA, USA). The SEM images were taken using a SEM (VEGA3, TESCAN, Busan, South Korea). Magnetization data were taken using a SQUID (MPMS-7, Quantum Design, Busan, South Korea). The elemental compositions of the hybrid catalysts were obtained using EDS (550i, IXRF Systems, Inc., Busan, South Korea), while the XRD patterns were recorded by a Rigaku RINT 2200 HK diffractometer (Rigaku Corporation, Tokyo, Japan). Mass spectra were obtained on a Shimadzu GC/MS, QP-2010 SE (EI) (Shimadzu Co., Kyoto, Japan). Reagents were purchased from Aldrich Chemical Co., TCI and Strem Chemical Co. and used as received without further purification. The concentration of 4-nitrophenol was determined at a wavelength of 400 nm using a SINCO S-3150 spectrophotometer (SINCO, Daejeon, Korea).

Figure 4. TEM images of Ag/Fe₃O₄, (a) before and (b) after the third cycles.



3.2. Synthesis of Fe₃O₄ Microspheres

Magnetite particles were synthesized using a solvothermal method [31]. The details were as follows: FeCl₃•6H₂O (0.36 g, 1.3 mmol) and trisodium citrate (Na₃Cit, 0.072 g, 0.24 mmol) were dissolved in ethylene glycol/ethanol (36 mL/4 mL) solution; then, sodium acetate (0.48 g, 5.9 mmol) was added under vigorous stirring for 10 min. The resulting mixture was then transferred to a Teflon-lined stainless-steel autoclave (with a capacity of 50 mL) for heating at 200 °C for 10 h. Then, the autoclave was carefully taken out and allowed to cool to room temperature. The as-made black products were thoroughly washed with ethanol three times, and they were then vacuum-dried.

3.3. Immobilization of Ag NPs onto Fe₃O₄ Microspheres

Ag NPs were immobilized onto Fe₃O₄ microspheres according to modified procedure of Yang *et al.* [31]. Fe₃O₄ microspheres were incubated in 0.2 M NaOH aqueous solution to ionize the carboxyl groups. The residual NaOH was removed by washing with deionized water through centrifugation. Then, the ionized Fe₃O₄ microspheres were dispersed in the solution (30 mL, 0.1 M) of AgNO₃ during 1 h under sonication. After this, the microspheres were harvested with the aid of the magnet and washed with deionized water three times. Then, the microspheres were redispersed in 20 mL of deionized water, and 50 mM NaBH₄ aqueous solution (1 mL) was added dropwise under ice water bath cooling during 5 min with vigorous stirring. The final product was purified through washing with water three times and dried under vacuum.

3.4. A Typical Procedure for Reduction of Nitroarenes

As a representative example, 7.50×10^{-4} M 4-nitrophenol solution and 0.026 mg of Ag/Fe₃O₄ [Ag base (17 wt%): 2.0 mol%] were mixed and sonicated for 30 s at room temperature. Then, 1.0 mL of 2.22 M NaBH₄ (300 equiv. to per equiv. of substrate) solution was added to the mixture. The reaction progress was monitored by UV/vis spectrometer.

3.5. A Typical Procedure for the Hydration of Nitriles

Ag/Fe₃O₄ catalyst (3.0 mol%), water (3.0 mL), and the corresponding nitrile (1.0 mmol) were introduced into a stainless steel reactor. After the reaction, the catalysts were separated from the solution by external magnet. The reaction products were analyzed by mass spectra on GC-MS. (Figures S1–S10).

3.5.1. GC-MS Data

Benzamide (Table 3, entry 5). To a stainless steel reactor equipped with magnetic stirrer were added benzonitrile 0.1 mL (1.0 mmol), Ag/Fe₃O₄ 19.0 mg (0.03 mmol) and H₂O (3 mL). The mixture was heated at 150 °C for 6 h. After cooling to room temperature, the solution was extracted with ethylacetate (20 mL). MS (EI) *m/z*: 28(100), 32(34), 51(30), 77(74), 105(75), 121(60).

4-Chlorobenzamide (Table 4, entry 1). 4-Chlorobenzonitrile (138 mg, 1.0 mmol) was hydrolysed as above. MS (EI) *m/z*: 75(33), 111(52), 139(100), 155(51).

4-Bromobenzamide (Table 4, entry 2). 4-Bromobenzonitrile (182 mg, 1.0 mmol) was hydrolysed as above. MS (EI) *m/z*: 28(27), 50(48), 139(100), 155(51), 183(100), 199(51).

4-nitrobenzamide (Table 4, entry 3). 4-nitrobenzonitrile (148 mg, 1.0 mmol) was hydrolysed as above. MS (EI) *m/z*: 28(100), 118(28), 150(78), 166(55).

4-aminobenzamide (Table 4, entry 4). 4-aminobenzonitrile (118 mg, 1.0 mmol) was hydrolysed as above. MS (EI) *m/z*: 28(100), 32(33), 65(29), 92(31), 120(75), 136(55).

4-Methylbenzamide (Table 4, entry 5). 4-Methylbenzonitrile (117 mg, 1.0 mmol) was hydrolysed as above. MS (EI) *m/z*: 28(85), 32(28), 65(25), 91(72), 119(100), 135(62).

3-methylbenzamide (Table 4, entry 6). 3-methylbenzonitrile (117 mg, 1.0 mmol) was hydrolysed as above. MS (EI) *m/z*: 65(26), 91(83), 119(100), 135(71).

2-methylbenzamide (Table 4, entry 7). 2-methylbenzonitrile (117 mg, 1.0 mmol) was hydrolysed as above. MS (EI) *m/z*: 65(33), 91(100), 119(87), 135(84).

Acetamide (Table 4, entry 8). acetonitrile (0.052 mL, 1.0 mmol) was hydrolysed as above. MS (EI) *m/z*: 28(100), 32(32), 44(77), 59(89).

Acrylamide (Table 4, entry 9). acrylonitrile (0.066 mL, 1.0 mmol) was hydrolysed as above. MS (EI) *m/z*: 27(75), 28(73), 32(17), 43(31), 74(83), 55(64), 71(100).

4. Conclusions

Ag NPs were immobilized onto Fe₃O₄ microspheres *in situ* by substituting sodium cations with Ag ions. The Ag NPs were uniformly immobilized in the Fe₃O₄ support while preserving their particle size and crystallinity, as well as the structural integrity of the Fe₃O₄ support. The Ag/Fe₃O₄ catalyzed the reduction of nitro compounds and hydration of nitriles to amides in water with high conversion. Furthermore, the Ag/Fe₃O₄ catalyst was readily separated using an external magnet and could be reused at least three times with benzonitrile under the optimized reaction conditions without any loss of catalytic activity. The magnetic separability eliminated the requirement of catalyst filtration after the completion of the reaction.

Supplementary Materials

Supplementary materials can be accessed at: <http://www.mdpi.com/1420-3049/19/1/699/s1>.

Acknowledgments

This research was supported by Basic Science Research Program through the National Research Foundation of Korea (NRF) funded by the Ministry of Science, ICT & Future Planning (No. 2013R1A1A1A05006634) and Ministry of Education (MOE) and National Research Foundation of Korea (NRF) through the Human Resource Training Project for Regional Innovation (No. 2012H1B8A2026225).

Conflicts of Interest

The authors declare no conflict of interest.

References

1. Kaneda, K.; Mitsudome, T.; Mizugaki, T.; Jitsukawa, K. Development of heterogeneous olympic medal metal nanoparticle catalysts for environmentally benign molecular transformations based on the surface properties of hydrotalcite. *Molecules* **2010**, *15*, 8988–9007.
2. Gan, N.; Hou, J.; Hu, F.; Zheng, L.; Ni, M.; Cao, Y. An amperometric immunosensor based on a polyelectrolyte/ gold magnetic nanoparticle supramolecular assembly-modified electrode for the determination of HIV p24 in serum. *Molecules* **2010**, *15*, 5053–5065.
3. Kamat, P.V. Meeting the clean energy demand: Nanostructure architectures for solar energy conversion. *J. Phys. Chem. C* **2007**, *111*, 2834–2860.
4. Steiner, D.; Mokari, T.; Banin, U.; Millo, O. Electronic structure of metal-semiconductor nanojunctions in gold CdSe nanodumbbells. *Phys. Rev. Lett.* **2005**, *95*, 056805.
5. Haruta, M.; Yamada, N.; Kobayashi, T.; Iijima, S. Gold catalysts prepared by coprecipitation for low-temperature oxidation of hydrogen and of carbon monoxide. *J. Catal.* **1989**, *115*, 301–309.
6. Chen, M.S.; Goodman, D.W. The structure of catalytically active Au on titania. *Science* **2004**, *306*, 252–255.
7. Wang, H.; You, T.; Shi, W.; Li, J.; Guo, L. Au/TiO₂/Au as a plasmonic coupling photocatalyst. *J. Phys. Chem. C* **2012**, *116*, 6490–6494.
8. Chen, S.; Si, R.; Taylor, E.; Janzen, J.; Chen, J. Synthesis of Pd/Fe₃O₄ hybrid nanocatalysts with controllable interface and enhanced catalytic activities for CO oxidation. *J. Phys. Chem. C* **2012**, *116*, 12969–12976.
9. Sun, S.; Murray, C.B.; Weller, D.; Folks, L.; Moser, A.A. monodisperse FePt nanoparticles and ferromagnetic FePt nanocrystal superlattices. *Science* **2000**, *287*, 1989–1992.
10. Miller, M.M.; Prinz, G.A.; Cheng, S.F.; Bounnak, S. Detection of a micron-sized magnetic sphere using a ring-shaped anisotropic magnetoresistance-based sensor: A model for a magnetoresistance-based biosensor. *Appl. Phys. Lett.* **2002**, *81*, 2211–2213.
11. Jain, T.K.; Morales, M.A.; Sahoo, S.K.; Leslie-Pelecky, D.L.; Labhasetwar, V. Iron oxide nanoparticles for sustained delivery of anticancer agents. *Mol. Pharm.* **2005**, *2*, 194–205.

12. Chourpa, I.; Douziech-Eyrolles, L.; Ngaboni-Okassa, L.; Fouquenot, J.F.; Cohen-Jonathan, S.; Souce, M.; Marchais, H.; Dubois, P. Molecular composition of iron oxide nanoparticles, precursors for magnetic drug targeting, as characterized by confocal Raman microspectroscopy. *Analyst* **2005**, *130*, 1395–1403.
13. Jang, Y.; Chung, J.; Kim, S.; Jun, S.W.; Kim, B.H.; Lee, D.W.; Kim, B.M.; Hyeon, T. Simple synthesis of Pd–Fe₃O₄ heterodimer nanocrystals and their application as a magnetically recyclable catalyst for Suzuki cross-coupling reactions. *Phys. Chem. Chem. Phys.* **2011**, *13*, 2512–2516.
14. Zhai, Q.-G.; Hu, M.-C.; Li, S.-N.; Jiang, Y.-C. Synthesis, structure and blue luminescent properties of a new silver(I) triazolate coordination polymer with 8²10-a topology. *Inorg. Chim. Acta* **2009**, *362*, 1355–1357.
15. Lee, D.; Cohen, R.E.; Rubner, M.F. Antibacterial properties of Ag nanoparticle loaded multilayers and formation of magnetically directed antibacterial microparticles. *Langmuir* **2005**, *21*, 9651–9659.
16. Luo, X.; Morrin, A.; Killard, A.J.; Smyth, M.R. Application of nanoparticles in electrochemical sensors and biosensors. *Electroanalysis* **2006**, *18*, 319–326.
17. Mitsudome, T.; Mikami, Y.; Funai, H.; Mizugaki, T.; Jitsukawa, K.; Kaneda, K. Oxidant-free alcohol dehydrogenation using a reusable hydrotalcite-supported silver nanoparticle catalyst. *Angew. Chem.* **2008**, *120*, 144–147.
18. Guan, Y.; Li, Y.; van Santen, R.A.; Hensen, E.J.M.; Li, C. Controlling reaction pathways for alcohol dehydration and dehydrogenation over FeSBA-15 catalysts. *Catal. Lett.* **2007**, *117*, 18–24.
19. Pradhan, N.; Pal, A.; Pal, T. Silver nanoparticle catalyzed reduction of aromatic nitro compounds. *Colloid. Surf. A-Physicochem. Eng. Asp.* **2002**, *196*, 247–257.
20. Cong, H.; Becker, C.F.; Elliott, S.J.; Grinstaff, M.W.; Porco, J.A., Jr. Silver nanoparticle-catalyzed Diels-Alder cycloadditions of 2'-hydroxychalcones. *J. Am. Chem. Soc.* **2010**, *132*, 7514–7518.
21. Narayanan, R.; El-Sayed, M.A. Catalysis with transition metal nanoparticles in colloidal solution: Nanoparticle shape dependence and stability. *J. Phys. Chem. B* **2005**, *109*, 12663–12676.
22. Motokura, K.; Fujita, N.; Mori, K.; Mizugaki, T.; Ebitani, K.; Kaneda, K. One-pot synthesis of α -alkylated nitriles with carbonyl compounds through consecutive aldol reaction/hydrogenation using a hydrotalcite-supported palladium nanoparticle as a multifunctional heterogeneous catalyst. *Tetrahedron Lett.* **2005**, *46*, 5507–5510.
23. Mori, T.; Watanuki, T.; Kashiwaguru, T. Diesel exhaust particles disturb gene expression in mouse testis. *Environ. Toxicol.* **2007**, *22*, 58–63.
24. Li, C.M.; Taneda, S.; Suzuki, A.K.; Furuta, C.; Watanabe, G.; Taya, K. Estrogenic and anti-androgenic activities of 4-nitrophenol in diesel exhaust particles. *Toxicol. Appl. Pharmacol.* **2006**, *217*, 1–6.
25. Pradhan, N.; Pal, A.; Pal, T. Catalytic reduction of aromatic nitro compounds by coinage metal nanoparticles. *Langmuir* **2001**, *17*, 1800–1802.
26. Esumi, K.; Isono, R.; Yoshimura, T. Preparation of PAMAM- and PPI-metal (silver, platinum, and palladium) nanocomposites and their catalytic activities for reduction of 4-nitrophenol. *Langmuir* **2004**, *20*, 237–243.

27. Zhang, P.; Shao, C.; Zhang, Z.; Zhang, M.; Mu, J.; Guoab, Z.; Liua, Y. *In situ* assembly of well-dispersed Ag nanoparticles (AgNPs) on electrospun carbon nanofibers (CNFs) for catalytic reduction of 4-nitrophenol. *Nanoscale* **2011**, *3*, 3357–3363.
28. Shimizua, K.; Imaiidab, N.; Sawabeb, K.; Satsuma, A. Hydration of nitriles to amides in water by SiO₂-supported Ag catalysts promoted by adsorbed oxygen atoms. *Appl. Catal. A-Gen.* **2012**, *421–422*, 114–120.
29. Mitsudome, T.; Mikami, Y.; Mori, H.; Arita, S.; Mizugaki, T.; Jitsukawa, K.; Kaneda, K. Supported silver nanoparticle catalyst for selective hydration of nitriles to amides in water. *Chem. Commun.* **2009**, 3258–3260.
30. Kim, A.Y.; Bae, H.S.; Park, S.; Park, S.; Park, K.H. Silver nanoparticle catalyzed selective hydration of nitriles to amides in water under neutral conditions. *Catal. Lett.* **2011**, *141*, 685–690.
31. Liu, B.; Zhang, W.; Yang, F.; Feng, H.; Yang, X. Facile method for synthesis of Fe₃O₄@Polymer microspheres and their application as magnetic support for loading metal nanoparticles. *J. Phys. Chem. C* **2011**, *115*, 15875–15884.
32. Hu, H.; Wang, Z.; Pan, L.; Zhao, S.; Zhu, S. Ag-coated Fe₃O₄@SiO₂ three-ply composite microspheres: Synthesis, characterization, and application in detecting melamine with their surface-enhanced raman scattering. *J. Phys. Chem. C* **2010**, *114*, 7738–7742.
33. Liu, P.; Zhao, M. Silver nanoparticle supported on halloysite nanotubes catalyzed reduction of 4-nitrophenol (4-NP). *Appl. Surf. Sci.* **2009**, *255*, 3989–3993.
34. Jana, S.; Ghosh, S.K.; Nath, S.; Pande, S.; Praharaj, S.; Panigrahi, S.; Basu, S.; Endo, T.; Pal, T. Synthesis of silver nanoshell-coated cationic polystyrene beads: A solid phase catalyst for the reduction of 4-nitrophenol. *Appl. Catal. A-Gen.* **2006**, *313*, 41–48.

Sample Availability: Samples of the compounds are available from the authors.

© 2014 by the authors; licensee MDPI, Basel, Switzerland. This article is an open access article distributed under the terms and conditions of the Creative Commons Attribution license (<http://creativecommons.org/licenses/by/3.0/>).